Available online at www.sciencedirect.com
ScienceDirect
Journal of Power Sources 158 (2006) 897–901
JOURNAL OF POWER SOURCES
www.elsevier.com/locate/jpowsour

Short communication

Microstructural analysis of new lead–acid electrode alloys

I. Mukaitani [a], H. Tsubakino [b,*], L. Liu [b], A. Yamamoto [b], S. Fukumoto [b]

[a] *Shin-Kobe Electric Machinery Co. Ltd., 1300-15 Yabata, Nabari, Mie 518-0625, Japan*
[b] *Division of Materials Science and Engineering, Graduate School of Engineering, University of Hyogo, 2167 Shosha, Himeji, Hyogo 671-2201, Japan*

Available online 5 July 2006

Abstract

The precipitation of Pb–0.08% Ca–1.5% Sn alloys with 0.04% Ag or 0.03% Bi additions was studied by resistivity measurements and transmission electron microscopy (TEM). The addition of Ag or Bi to the Pb–Ca–Sn ternary alloys suppresses discontinuous precipitation and accelerates the formation of continuous precipitates with high coherency strain. Ag addition has a greater effect on hardening than Bi addition. TEM-energy dispersive spectroscopy (EDS) analysis confirmed that the continuous precipitates formed in Ag-supplemented alloys contain Ag in addition to Ca, Sn and Pb elements.

Keywords: Lead alloy; Addition; Precipitation; Microstructure; Resistivity; Transmission electron microscopy

1. Introduction

The precipitation of Pb_3Sn from a supersaturated α-solid solution in Pb–Ca binary alloys is known to cause significant age hardening [1–3]. This hardening occurs by discontinuous precipitation [4–8]. Commercial Pb–Ca alloys for maintenance-free storage batteries contain Sn [9]. The effect of Sn addition on precipitation in Pb–Ca binary alloys has also been studied [10–12]. Borchers and Assmann [10] found by metallographic and hardness measurements that the addition of Sn retarded discontinuous precipitation and that continuous precipitation occurred preferentially when Sn additions exceeded the atom quantity of Ca by three-fold. Tsubakino et al. [11] reported by electrical resistivity and transmission electron microscopy (TEM) that Sn addition retarded discontinuous precipitation and that continuous precipitation occurred preferentially for higher Sn contents, with the amount of Sn necessary for retardation higher for higher Ca contents. Precipitates in the Pb–Ca–Sn ternary alloy have an $L1_2$-type (Cu_3Au) ordered structure, Pb_3Ca [12], Sn_3Ca [10] or $(Pb,Sn)_3Ca$ [7,13].

To improve the corrosion resistance and creep strength of maintenance-free electrodes, Ag and/or Bi are added to the Pb–Ca–Sn ternary alloy, with Ag addition effectively acting to increase the electrochemical and mechanical properties [7,14–16]. However, there is no detailed information on microstructural studies of aged Pb–Ca–Sn–Ag (or Bi) alloys.

In the present study, the precipitation process during aging was studied by means of electrical resistance measurements and TEM observations to clarify the effect of Ag (or Bi) additions on precipitation in Pb–Ca–Sn ternary alloys.

2. Experimental procedure

The alloys used in this study were prepared from Pb (99.99%), Pb–2.7% Ca mother alloy, Sn (99.99%), Ag (99.99%) and Bi (99.99%). They were melted together and cast into an iron mold. The chemical compositions of the alloys are shown in Table 1 [the nominal mass % used was: Pb, 0.06–0.1; Ca, 1.0–2.0; Sn, 0.04 Ag (or 0.03 Bi)]. The ingots were homogenized at 573 K for 396 ks. The specimens for metallographic and hardness measurements were plates of approximately $10 \times 5 \times 3\,mm^3$ and the specimens for electrical resistivity were wires of 1.8 mm in diameter and approximately 65 mm in length.

Specimens were solution-annealed at 573 K for 3.6 ks, quenched in iced water and then aged isothermally at 333 K. Hardness was measured with a micro-Vickers hardness tester, applying 0.245 N. The resistance of the specimens during aging was measured using a four-probe potentiometric technique. The specimens were held in liquid nitrogen during measurements. The foils for TEM observations were prepared by twin-jet electro-polishing using 60% $HClO_4$–40% H_2O solution and subsequent milling using argon–ion plasma [13]. The foils were

* Corresponding author. Tel.: +81 792 67 4901; fax: +81 792 67 4901.
E-mail address: Tsubakino@eng.u-hyogo.ac.jp (H. Tsubakino).

0378-7753/$ – see front matter © 2006 Published by Elsevier B.V.
doi:10.1016/j.jpowsour.2006.05.013

Table 1
Chemical composition of alloys (mass%)

Alloy		Ca	Sn	Ag	Bi
I	Pb–0.06Ca–1.0Sn	0.057	0.997		
	Pb–0.06Ca–1.6Sn	0.06	1.7		
	Pb–0.06Ca–2.0Sn	0.057	2.079		
	Pb–0.08Ca–1.0Sn	0.085	1.036		
	Pb–0.08Ca–1.6Sn	0.083	1.727	<0.001	<0.005
	Pb–0.08Ca–2.0Sn	0.083	2.098		
	Pb–0.10Ca–1.0Sn	0.099	1.007		
	Pb–0.1 Ca–1.6Sn	0.106	1.723		
	Pb–0.1 Ca–2.0Sn	0.113	2.092		
II	Pb–0.08Ca–1.5Sn	0.076	1.5		
	Pb–0.08Ca–1.5Sn–0.04Ag	0.079	1.5	0.039	
	Pb–0.08Ca–1.5Sn–0.03Bi	0.082	1.5		0.029

examined in a JEM 2010 electron microscope with an energy-dispersive X-ray spectroscopic (EDS) analysis system, operated at 200 kV.

3. Results and discussion

3.1. Resistivity

Typical resistivity curves with aging time for the ternary alloys are shown in Figs. 1 and 2. In these figures, the variations in relative resistivity, ρ/ρ_0, are plotted against aging time, where ρ and ρ_0 are the resistivity at aging time t and of as-quenched specimens, respectively. The resistivity decreases in a single stage, which is similar to that for alloys with Ca content lower than 0.04% [11]. These resistivity changes are very similar, even for various Ca and Sn contents within this study. Therefore, the precipitation behavior in these ternary alloys is almost the same, irrespective of different Ca and Sn contents. The decrease in the resistivity curves is attributed to the formation of continuous precipitates; a similar precipitation mode in ternary alloys was reported by Bouirden et al. [7] using hardness measurements and by Muras et al. [12] from TEM observations.

Typical resistivity changes in alloys with added Ag or Bi are shown in Fig. 3. Bi addition to the ternary alloy did not affect the resistivity change of the ternary alloy, but Ag addition led to a faster decrease in resistivity and a greater total resistivity change. These results mean that Ag addition increases the precipitation rate and the degree of super-saturation of solute elements in the matrix, but Bi addition does not.

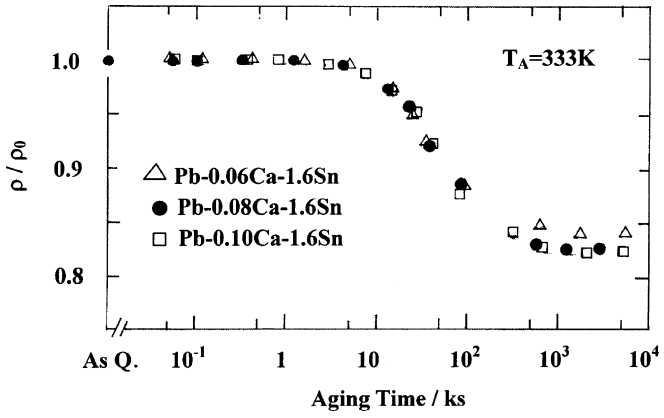

Fig. 1. Typical resistivity curves during aging at 333 K in Pb–1.6% Sn alloys with various Ca contents.

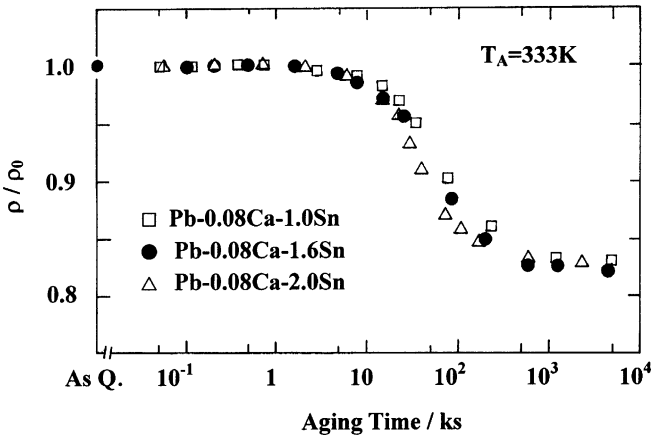

Fig. 2. Typical resistivity curves during aging at 333 K in Pb–0.08% Ca alloys with various Sn contents.

3.2. Microstructure and hardness

Typical optical micrographs are shown in Fig. 4. Microstructural changes accompanying the aging of Pb–Ca–Sn ternary alloys (Fig. 4a) are essentially similar to those in our previous study [11], i.e., very narrow, discontinuous precipitation cells at grain boundaries were observed, even after prolonged aging at 333 K. Therefore, this study has confirmed that the retarding phenomena of discontinuous precipitation are caused by the addition of Sn to Pb–Ca binary alloys (Fig. 4a). Additions of Ag and Bi cause much greater retarding effects on cell advance, resulting in smooth grain boundaries (Fig. 4b and c). Therefore, additions of Ag and Bi introduce a larger grain size than that in the Pb–Ca–Sn ternary alloys, although the alloy with added Bi shows a slightly smaller grain size compared to the

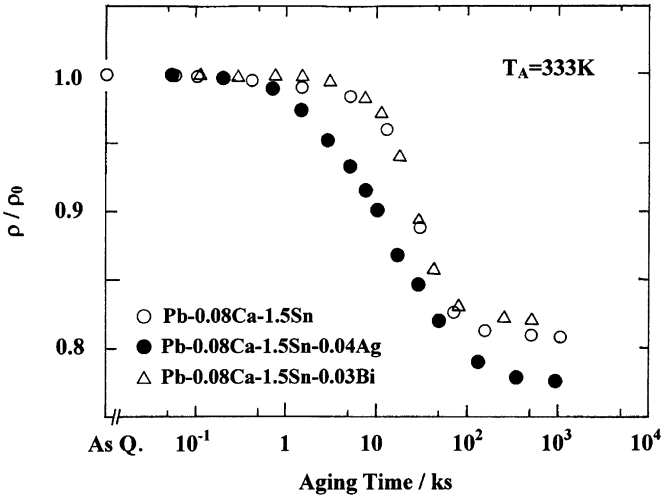

Fig. 3. Typical resistivity curves during aging at 333 K in Pb–0.08% Ca–1.5% Sn, and 0.04% Ag or 0.03% Bi alloys.

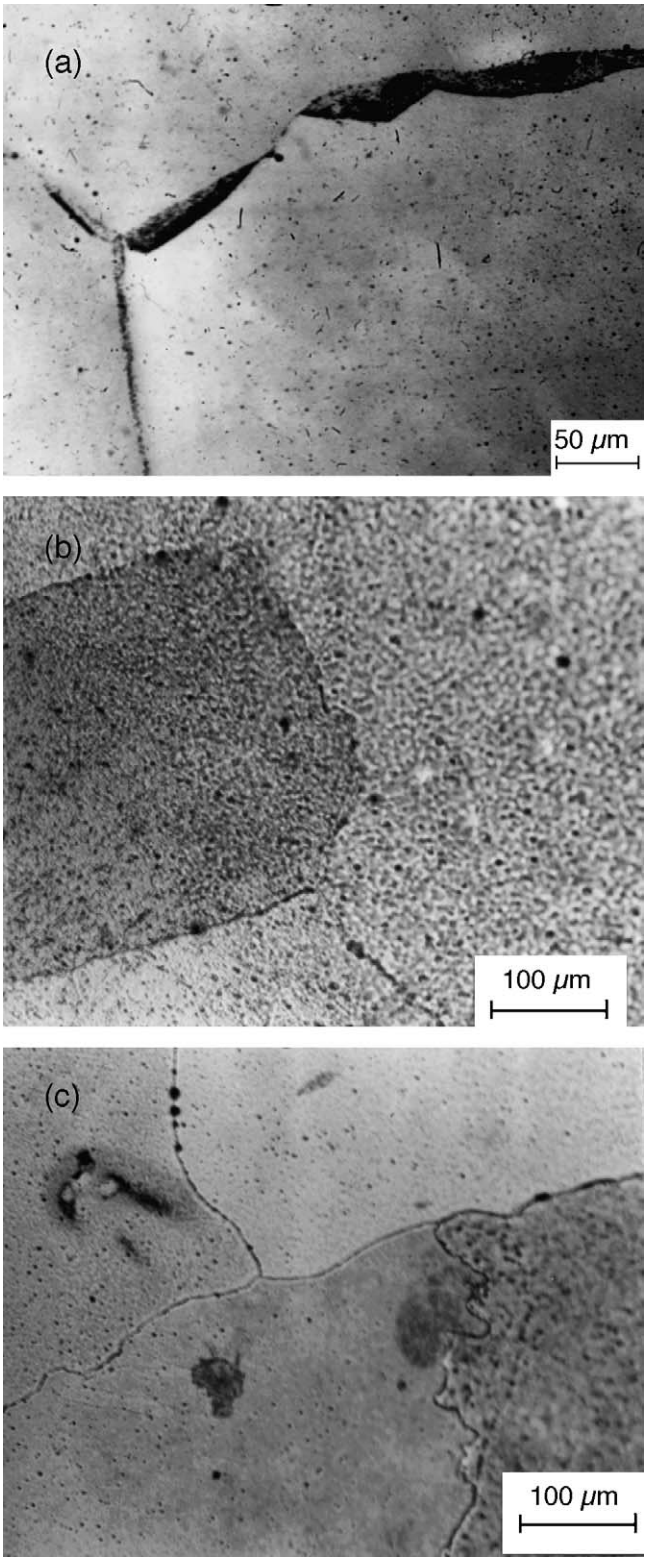

Fig. 4. Typical microstructures in (a) Pb–0.08% Ca–1.5% Sn, (b) Pb–0.08% Ca–1.5% Sn–0.04% Ag and (c) Pb–0.08% Ca–1.5% Sn–0.03% Bi alloys aged at 333 K for 86.4 ks.

Ag-supplemented alloy. These additives lead to an improvement in the corrosion resistance of Pb–Ca–Sn alloys, because corrosion generally occurs at grain boundaries and much improved corrosion resistance is expected with increasing grain size [17].

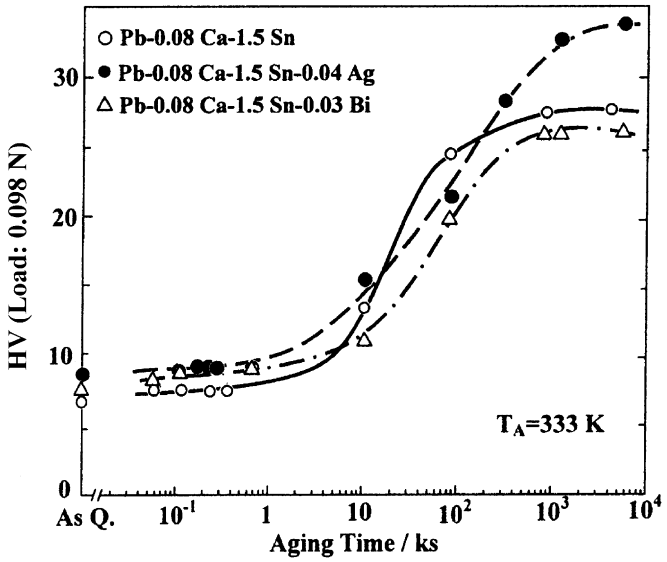

Fig. 5. Age hardening curves at 333 K in Pb–0.08% Ca–1.5% Sn alloys containing 0.04% Ag or 0.03% Bi.

We conclude again that precipitation in the alloys used in this study occurred mainly via a continuous mode.

Typical age-hardening curves measured in grain interiors are shown in Fig. 5. Bi and Ag additions led to a slight increase in the as-quenched hardness, presumably due to solid solution hardening. The hardness curve for the alloy with added Bi does not differ much from that for the ternary alloy, but the Ag-supplemented alloy shows a much higher value for maximum hardness. These hardness curves correspond well with the resistivity curves shown in Fig. 3. The present results suggest that Ag addition will induce a higher coherent strain around continuous precipitates with higher density. A similar increase in mechanical properties on the addition of Ag was reported by Prengaman [14], although the increase was small because the author used a Pb–0.04 Ca–1.1 Sn alloy with 0.02–0.05% Ag and the aging was carried out at room temperature.

3.3. Precipitation kinetics

The time dependence of the fraction (f) of precipitation at constant temperature is expressed by the Johnson–Mehl [18] equation:

$$f = 1 - \exp(-bt^n) \tag{1}$$

where t is aging time, and b and n are constants.

From resistivity measurements, the fraction f of precipitation is taken to be:

$$f = \frac{(\rho_0 - \rho)}{(\rho_0 - \rho_f)} \tag{2}$$

where ρ_f is the final value of ρ.

The relationship between $\log\log\{1/(1-f)\}$ and $\log t$ is shown in Fig. 6. From the slope, the value of n was obtained. The n values for ternary and Bi-supplemented alloys are almost the same, but the n-value for the alloy with added Ag tended to decrease, although the value is close to that for the ternary

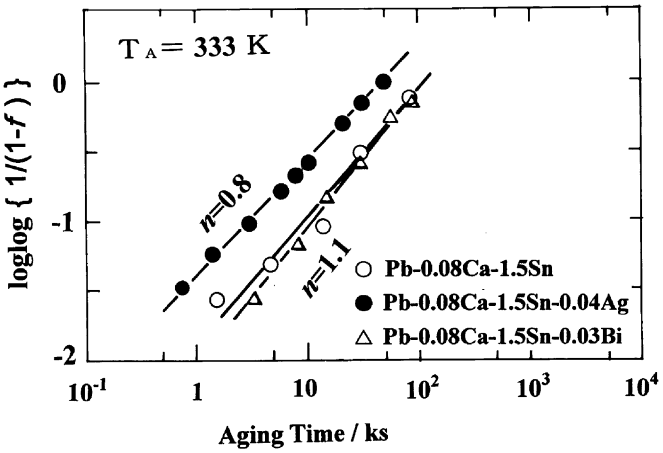

Fig. 6. Plots of loglog{1/(1 −*f*)} vs. aging time.

alloys, in the range 0.8–1.1. According to Christian [19], $n = 2/3$ implies precipitation on dislocations, $n = 1$ indicates the formation of cylinder-shaped precipitates and $n = 1.5$ means spherical precipitates in a homogeneous reaction.

3.4. Continuous precipitates

A TEM micrograph of the alloy with added Ag aged at 343 K for 4 Ms is shown in Fig. 7. Many continuous precipitates with a butterfly-type strain field contrast can be clearly observed in Fig. 7a. Borchers and Assmann, using an extraction technique [10], reported plate-like continuous precipitates of Sn_3Ca aligned in the [100] direction in a Pb – 0.06%, Ca – 0.7%, Sn alloy aged at 423 K for 2.2 Ms. However, the strain contrasts observed in this study indicate the formation of spherical precipitates, i.e., coherent elastic strain around the interfaces of small spherical precipitates was observed [20]. The precipitate size is small as approximately 10 nm in diameter. Comparison of the TEM micrograph for the alloy with added Bi (Fig. 7b) with that for added Ag shows much finer and higher density continuous precipitates.

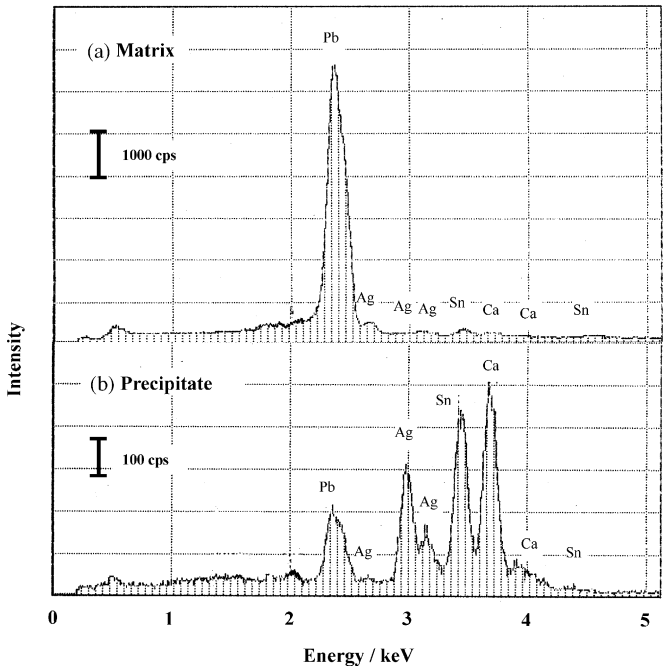

Fig. 8. TEM-EDS spectra of (a) matrix and (b) continuous precipitates in Pb–0.08%, Ca–1.5%, Sn–0.04%, Ag aged at 333 K for 3 Ms.

TEM-EDS analysis was performed to estimate the composition of the continuous precipitates. The diameter of the concentrated incident electron beam on the foil surface for analysis was smaller than the precipitates in this study, but the X-ray spectrum could be expected to originate from both the precipitates and the matrix. Therefore, analysis was performed as far as possible on large precipitates. Typical TEM-EDS spectra for such precipitates and the matrix are shown in Fig. 8. The continuous precipitates formed in the Pb–Ca–Sn ternary alloys were $L1_2$-type ordered Pb_3Ca [12] or $(Pb,Sn)_3Ca$ [7,13]. The precipitates undoubtedly consist of Ag, in addition to Ca, Sn and Pb elements, in the alloy with added Ag, although the actual composition of precipitates was not obtained because of matrix effects in the spectra. The precipitates formed in the Pb–Ca–Sn

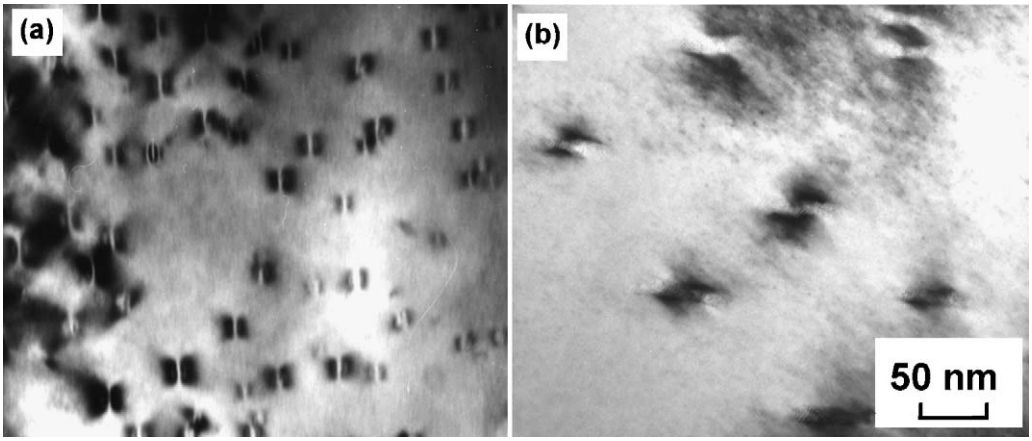

Fig. 7. Typical TEM image showing continuous precipitates. (a) Pb–0.08%, Ca–1.5%, Sn–0.04%, Ag alloy aged at 333 K for 4 Ms; and (b) Pb–0.08%, Ca–1.5%, Sn–0.03%, Bi alloy aged at 333 K for 3 Ms.

alloy with added Ag are probably $(Pb,Sn)_3Ca$ containing Ag. Moreover, the precipitation rate was much faster for the Ag-supplemented alloy than for the ternary alloy, as shown in Fig. 3. Thus, Ag atoms act as nuclei for the formation of continuous precipitates, resulting in the acceleration of continuous precipitation nucleation, but Bi does not. Furthermore, an increase in the number of continuous precipitates with high coherency was observed in TEM micrographs, which led to greater hardening, as shown in Fig. 5. Thus, the addition of Ag can suppress discontinuous precipitation because of the acceleration of continuous precipitation. Prengaman [14] reported that Ag segregated at grain boundaries. Such Ag segregation would act to suppress cell advance in discontinuous precipitation in addition to the occurrence of continuous precipitation; however, Ag segregation at grain boundaries cannot be confirmed in this study.

The acceleration effects due to continuous precipitation on the addition of Ag to ternary Pb–Ca–Sn alloys is an important factor that may improve the creep strength.

4. Summary

(1) Precipitation in the alloys in this study occurred by a few discontinuous precipitation cells and preferentially by continuous precipitation. The sequence and precipitation rate in Pb–Ca–Sn ternary alloys were almost the same, irrespective of different Ca and Sn contents.
(2) Addition of Ag to Pb–Ca–Sn ternary alloys retarded discontinuous precipitation and accelerated continuous precipitation, resulting in remarkable hardening, but Bi did not.
(3) In the alloy with added Ag, continuous precipitation occurred, with fine precipitates of high density and high coherent strain. Elemental Ag, in addition to Ca, Sn and Pb elements, was present in the continuous precipitates formed in the Ag-supplemented alloy. Thus, added Ag formed nuclei for continuous precipitates, resulting in an increase in density of the precipitates and in age hardening.

Acknowledgements

The authors are grateful to students Mr. S. Masumoto, Ms. A. Yamaguchi and Ms. S. Ashida for their experimental efforts in this study. Thanks also to Mr. S. Ioku in the TEM laboratory for taking TEM micrographs.

References

[1] E.E. Schumacher, G.M. Bouton, Met. Alloys 1 (1930) 405–409.
[2] W. Hofmann, Blei und Bleilegierungen, Springer-Verlag, Berlin, 1962, pp. 23–104.
[3] M. Myers, H.R. Van Handle, C.R. DiMartini, J. Electrochem. Soc. 121 (1974) 1526–1530.
[4] H. Scharfenberger, S. Henkel, Z. Metallkd. 64 (1973) 478–483.
[5] H. Borchers, W. Schafenbergers, W. Henkel, Z. Metallkd. 66 (1975) 111–118.
[6] H. Tsubakino, R. Nozato, Y. Satoh, Z. Metallkd. 81 (1990) 490–495.
[7] L. Bouirden, J.P. Hilger, J. Herz, J. Power Sources 33 (1991) 27–50.
[8] H. Tsubakino, R. Nozato, A. Yamamoto, Z. Metallkd. 84 (1993) 29–32.
[9] J. Perkins, G.R. Edwards, J. Mater. Sci. 10 (1975) 136–158.
[10] H. Borchers, H. Assmann, Z. Metallkd. 69 (1978) 43–49.
[11] H. Tsubakino, M. Tagami, S. Ioku, A. Yamamoto, Metall. Mater. Trans. A 27A (1996) 1675–1682.
[12] L. Muras, P.R. Munroe, S. Blairs, P. Kraukis, Z.W. Chen, J.B. See, J. Power Sources 55 (1995) 119–122.
[13] H. Tsubakino, R. Nozato, A. Yamamoto, Scr. Metall. Mater. 26 (1992) 1681–1685.
[14] R.D. Prengaman, J. Power Sources 67 (2001) 267–278;
R.D. Prengaman, J. Power Sources 95 (2001) 224–233.
[15] S. Zhong, H.K. Liu, S.X. Dou, M. Skyllas-Kazacob, J. Power Sources 59 (1996) 123–129.
[16] L. Albert, A. Chabrol, L. Torcheux, P. Steyer, J. Power Sources 67 (1997) 257–265.
[17] D.A.J. Rand, D.P. Boden, C.S. Lakshmi, R.F. Nelson, R.D. Prengaman, J. Power Sources 107 (2002) 280–300.
[18] W.A. Johnson, R.F. Mehl, Trans. AIME 139 (1939) 416–441.
[19] J.W. Christian, The Theory of Transformation in Metals and Alloys, Pergamon Press, Oxford, 1965, pp. 471–495.
[20] P.G. Hirch, A. Howie, R.B. Nicholoson, D.W. Pashley, M.J. Whelan, Electron Microscopy of Thin Crystals, Butterworths, London, 1986, pp. 156–194.